Journal of Theoretical
and Applied Mechanics
Sofia, 1992, Year XXIII, No 2

L. Hitova
E. Trifonova

Chemical Mass Transport and Epitaxial Growth of Semiconductor Materials

The interest in GaAs- and InAs-based solid solutions (GaInAs, GaInAsP) has increased rapidly over the past five years. It has been stimulated by the success in fabricating monocrystal layers of high structural perfection. One of the most promising growth methods is the combination of chemical mass transport and epitaxial deposition.

In the present work we report our results on the production and the study of the structures InAs/GaAs, InAs/InAs and GaAs/GaAs [1-8]. The system $InAs\text{-}AsCl_3\text{-}H_2$ has been studied in detail. The results are also valid for GaAs.

The source material for epitaxial growth was GaAs (or Ga) and InAs, synthesized beforehand by direct interaction of the melted components in stoichiometric ratio. Iodidely synthesized InAs has also been used. The transporting agent was 6-7 N pure $AsCl_3$. The carrier gas, hydrogen, was Pd-diffused and contained ~ 0,5 ppm O_2. The (111)A-, (111)B- and (100)- oriented substrates of GaAs and InAs were chemically-mechanically polished, chemically etched and, prior to epitaxial growth, etched "*in situ*" by $AsCl_3$ + H_2.

The effect of the technology parameters (source and substrate temperatures, $AsCl_3$ mole fraction, X_{AsCl_3}, carrier gas mobility, V^o, substrate orientation, etc.) on chemical transport and epitaxial growth rates, electrical parameters and structure of the layers was studied. Optimal transport and growth regimes were evaluated on the basis of preliminary thermodynamic calculations of equilibrium partial pressures of the gaseous species ($InCl_3$, $InCl_2$, HCl, $AsCl_3$, As_2, In_2Cl_3, In_2Cl_6, As_4, InCl, H_2) at given temperatures and X_{AsCl_3}. The calculations showed that the partial pressures of the gaseous species grow with the increase of $Q = [Cl]/[H]$. The highest partial pressure is that of InCl; it reaches saturation at $T \geq 700^{o}C$, due to complete interaction of the source InAs with the gas phase. Since In_2Cl_3 and $InCl_2$ partial pressures are higher than that of $InCl_3$, the deposition of InAs may be presented by the reaction:

$$3InCl_{(g)} + 1/4As_{4(g)} = InAs_{(s)} + In_2Cl_{3(g)}.$$

The calculated partial pressures were used for evaluation of the thermodynamic transport and growth rates of InAs. These were compared with experimental data.

The dependences of the transport rate on X_{AsCl_3}, V^o and T_{source} are presented in Figs 1-3. The last dependence is a weak one which is in agreement with the thermodynamically predicted saturation of the hypothetical partial pressure of InAs at $T \geq 700^{o}C$. The decrease of the source quantity with time shows that the complex reaction of InAs and the gas phase takes place as a pseudomonomolecular process.

From the results presented so far, it can be concluded that the source and the gas phase are in near-equilibrium interaction. The thermodynamic model is adequate to the processes in the source zone, which are independent of the conditions of epitaxial growth in the substrate zone.

The investigations on the kinetics of homo- and heteroepitaxy of InAs show that depending on $T_{substr.}$ and X_{AsCl_3}, the growth may proceed in either thermodynamically or kinetically controlled regimes (Figs 4-6). The dependence of the deposition rate on substrate orientation varies with X_{AsCl_3}. The temperatures, corresponding to maximal growth rates shift towards lower values with X_{AsCl_3} increasing. The deviation of experimental growth rates from calculated ones can be used to evaluate the deviation of the system in the substrate zone from equilibrium. The growth rate is limited by the interaction (adsorption, chemical reaction, desorption) of the substrate and the gas phase; the rate increases with temperature increasing. The activation energies are approx. 100 kJ mol^{-1} and 220 kJ mol^{-1} for homo- and heteroepitaxy of InAs. These values confirm the kinetic control of growth at low temperatures.

The layer thickness D as a function of growth duration t is shown in Fig.7. $D = k.t$ (where k is the growth rate, $\sim 10\ \mu m\ h^{-1}$) is the kinetic equation of the total reaction of InAs growth. Consequently, this reaction is of a zeroth order under the conditions of a kinetically controlled process.

The growth rate increases with T_{source} increasing, reaching maximum.

Theoretical and experimental efficiencies of InAs transport as functions of Q and T are presented in Fig.8 and Fig.9. The experimental data follow the calculated curve at $T \geq 800^{o}C$. Hence, a further increasing of T_{source} is not necessary; it would only result in a greater contamination of the system.

The efficiency of the epitaxial growth is greater in the case of homoepitaxy. The difference decreases with temperature increasing (Fig.10).

The surface morphology of the layers is better when growth takes place in thermodynamically controlled regimes. In general, it depends on growth temperature and X_{AsCl_3}. The dislocation density N_D at the surface of homoepitaxial InAs layers is lower than that in of substrate material. The distribution of N_D through the layer thickness was studied on InAs/GaAs structures (Fig.11). The increasing of N_D in the contact region is due to misfit dislocations. The decreasing part of the curve is of greater interest as it shows that after a "critical" thickness N_D decreases with thickness increasing. N_D depends on X_{AsCl_3} (Fig. 12), and, consequently, on current carriers concentration (Fig.13). This results in the supposition that the decreasing of N_D is due to "pinning" of dislocations at impurity atoms which form stronger bonds with host In or As atoms than the bond In-As, an effect already known for bulk GaAs and InP crystals.

Semiinsulating Cr-doped GaAs substrates were used to investigate the dependences of electrical parameters of InAs layers on technology conditions. As it can be seen in Fig.14, the current carriers mobilities increase and the carriers concentrations decrease with X_{AsCl_3} increasing, an effect which is known for GaAs growth. The same is valid also for the system with iodidely synthesized InAs source. The effect is connected with the elimination of certain impurities.

References

1. Hitova, L., E. P. Trifonova. Effect of the $AsCl_3$ mole fraction on the electrical parameters of vapour grown heteroepitaxial indium arsenide layers. — Thin Solid Films, **52**, 1978, 397-403.
2. Trifonova, E. P., L. Hitova. Effects of the $AsCl_3$ mole fraction and the substrate orientation on the electrical parameters of heteroepitaxial indium arsenide layers. — Thin Solid Films, **65**, 1980, 61-66.
3. Hitova, L., E. P. Trifonova. Growth kinetics and surface morphology of homoepitaxial indium arsenide layers. — Vide, Couches Minces, Suppl., **201**, 1980, 153-156.
4. Trifonova, E. P., L. Karagiozov, L. Hitova. Application of the iodide synthesis to the preparation of indium arsenide bulk crystals and epitaxial layers. — Cryst. Res. Technol., **18**, 1983, 1341-1346.
5. Hitova, L., E. P. Trifonova, I. N. Kishmar, M. Apostolova. Physico - chemical analysis of InAs gas phase epitaxy in the InAs - $AsCl_3$ - H_2 system. I: Thermodynamic considerations. — Thin Solid Films, **147**, 1987, 33-40.

6. Trifonova, E. P., L. Hitova. Physico-chemical analysis of InAs gas phase epitaxy in the InAs-$AsCl_3$-H_2 system. II: InAs transport and epitaxial growth kinetics. — Thin Solid Films, **147**, 1987, 41-48.
7. Trifonova, E. P., L. Hitova. Efficiencies of InAs transport and epitaxial growth by chemical vapour deposition in the system InAs-$AsCl_3$-H_2. — Thin Solid Films, **161**, 1988, 257-261.
8. Trifonova, E. P., L. Hitova. Dislocation density in heteroepitaxial InAs layers. — Cryst. Res. - Technol., **25**, 1990, 693-698.

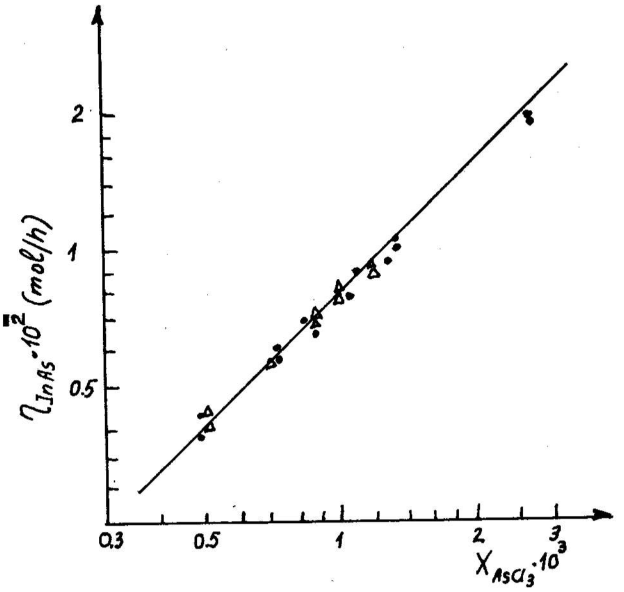

Fig.1. InAs transport rate *vs.* X_{AsCl_3} at $T_{source} = 800^{\circ}C$.

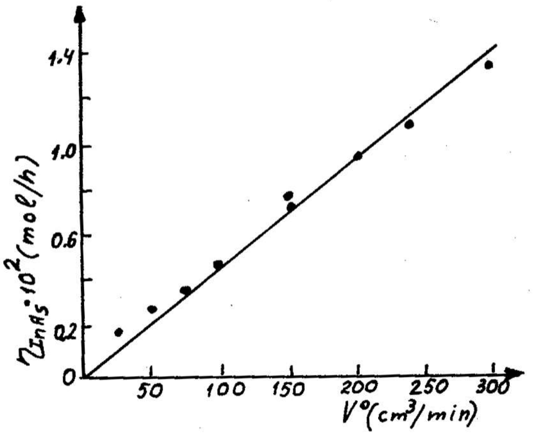

Fig.2. InAs transport rate *vs.* V°.

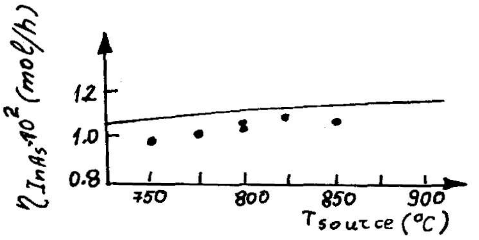

Fig.3. InAs transport rate *vs.* T_{source}.

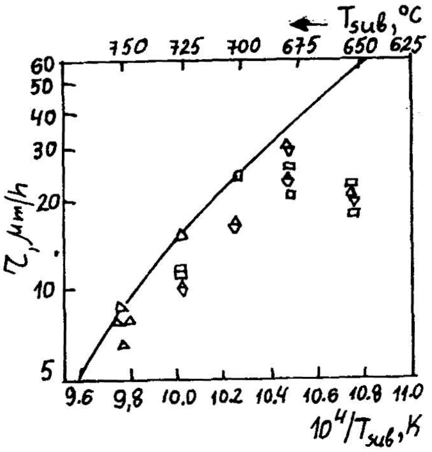

Fig.4. InAs/InAs growth rate *vs.* $T_{substr.}$ at T_{source} = 800°C, X_{AsCl_3} = 1.0 x 10^{-3}, V^o = 240 cm^3min^{-1}.

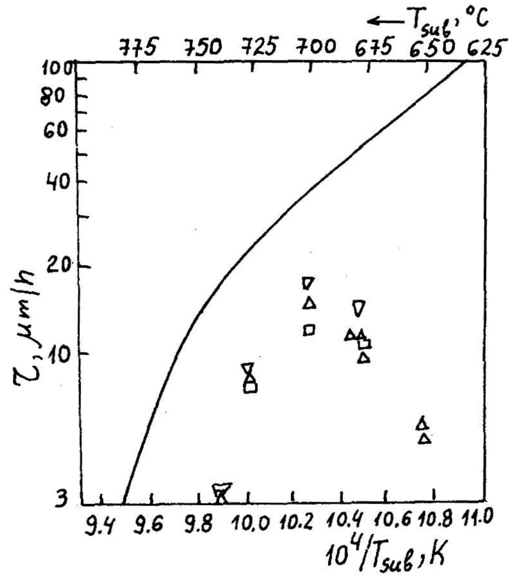

Fig.5. InAs/GaAs growth rate *vs.* $T_{substr.}$ at T_{source} = 800°C, X_{AsCl_3} = 1.4 x 10^{-3}, V^o = 240 cm^3min^{-1}.

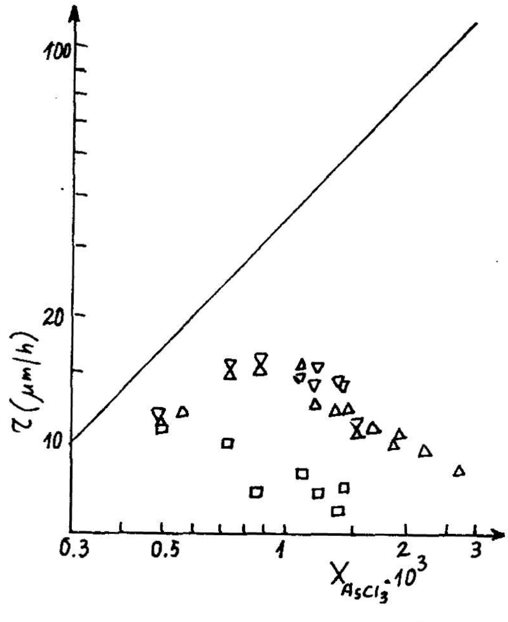

Fig.6. InAs/GaAs growth rate *vs.* X_{AsCl_3} at T_{source} = 800°C, $T_{substr.}$ = 675°C, V^o=240 cm^3min^{-1}.

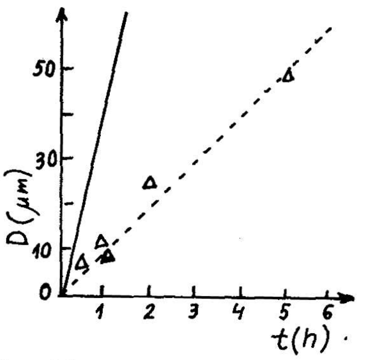

Fig.7. Time dependence of D on GaAs(111)B at T_{source} = 800 °C, $T_{substr.}$ = 675°C, X_{AsCl_3} = 1.4 x 10^{-3}, V^o = 240 $cm^3 min^{-1}$.

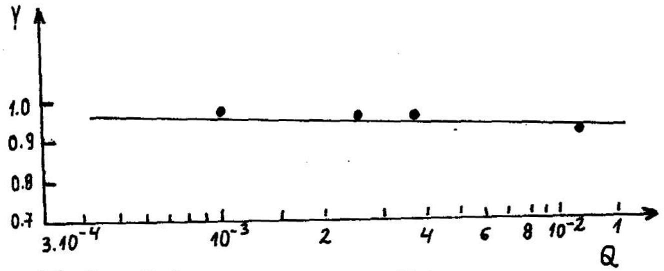

Fig.8. InAs transport efficiency *vs.* Q for T_{source} = 800°C.

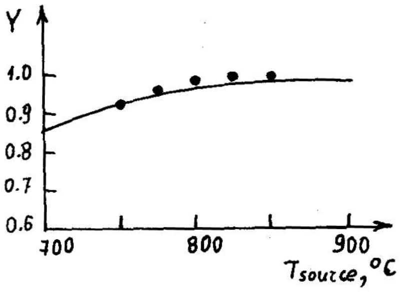

Fig.9. InAs transport efficiency *vs.* T for Q = 7 x 10^{-3}

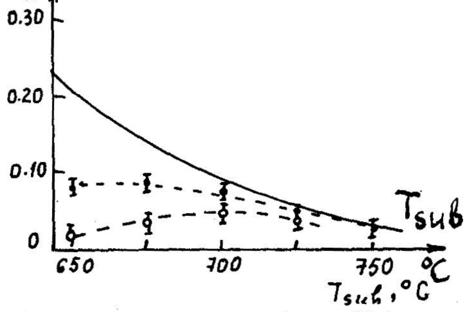

Fig.10. InAs growth efficiency on InAs and GaAs *vs.*$T_{substr.}$.

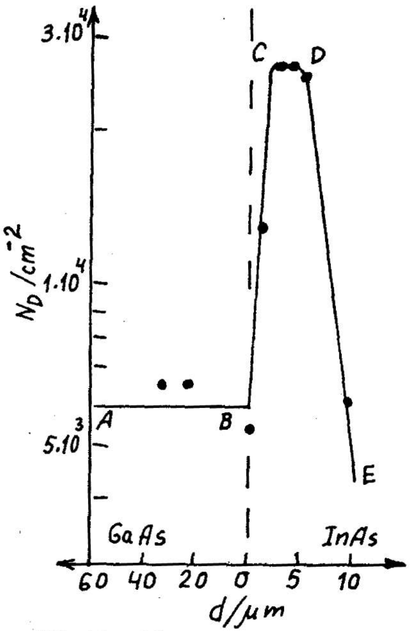

Fig.11. N_D vs. D ($T_{substr.}$=700°C, $XAsCl_3$=1.29 x 10^{-3}).

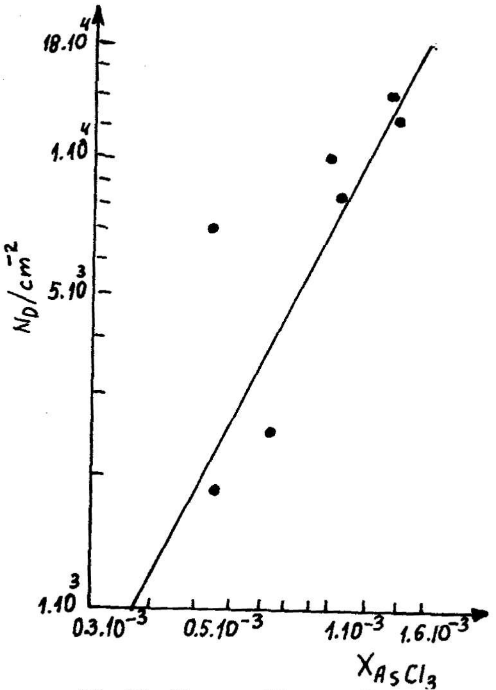

Fig.12. N_D vs. $XAsCl_3$ (D = 7 μm).

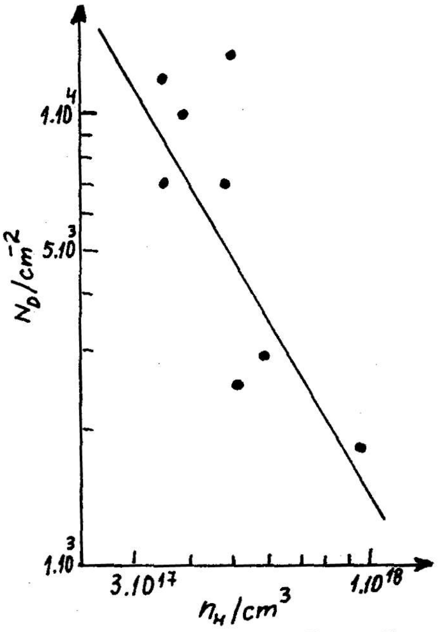

Fig.13. N_D vs.n_{H300K} (D = 7 μm).

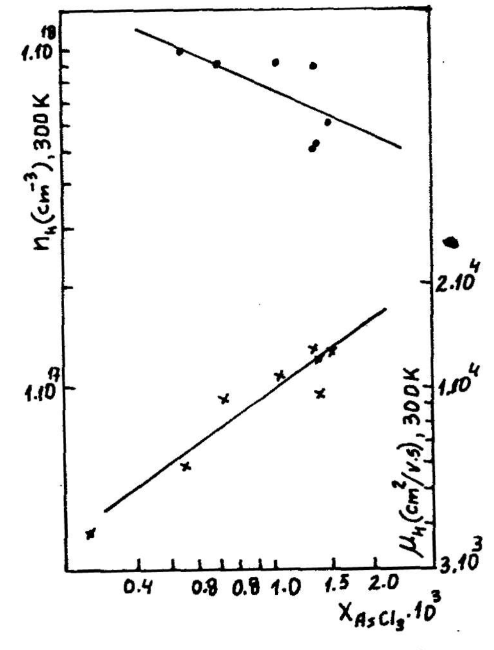

Fig.14. Dependence of n_H and μ_H on $XAsCl_3$ at 300K.